Monte Carlo modeling of geminate recombination in polymer-polymer photovoltaic devices

C. Groves, R. A. Marsh, and N. C. Greenham

Citation: The Journal of Chemical Physics **129**, 114903 (2008); doi: 10.1063/1.2977992
View online: http://dx.doi.org/10.1063/1.2977992
View Table of Contents: http://scitation.aip.org/content/aip/journal/jcp/129/11?ver=pdfcov
Published by the AIP Publishing

Monte Carlo modeling of geminate recombination in polymer-polymer photovoltaic devices

C. Groves,[a] R. A. Marsh, and N. C. Greenham
Cavendish Laboratory, Cambridge University, JJ Thomson Avenue, Cambridge CB3 OHE, United Kingdom

(Received 22 April 2008; accepted 12 August 2008; published online 17 September 2008)

A Monte Carlo model is used to examine geminate pair dissociation in polymer-polymer photovoltaic devices. It is found that increasing one or both carrier mobilities aids geminate separation yield η_{GS} particularly at low fields. This, in turn, leads to improved maximum power output from polymer-polymer blend photovoltaics, even when carrier mobilities are unbalanced by a factor of 10. The dynamic behaviors of geminate charges that eventually separate and recombine are examined for the first time. It is shown that geminate pairs in a bilayer become effectively free when separated by ~4 nm, which is far smaller than the thermal capture radius of 16 nm here. This may lead one to expect that η_{GS} would not be limited by the separation allowed by the morphology once the domain size has increased above 4 nm. In fact it is found that η_{GS} in a blend improves continuously as the average domain size increases from 4 to 16 nm. We show that although a small degree of separation may be available in a blend, the limited number of possible routes to further separation makes charge pairs in blends more susceptible to recombination than charge pairs in a bilayer. © *2008 American Institute of Physics*. [DOI: 10.1063/1.2977992]

INTRODUCTION

In order for organic polymer-polymer photovoltaic devices (OPVs) to realize their potential as cheap, large-area harvesters of solar energy, their power conversion efficiency η_P must be improved above the current best result of ~1.8%.[1–3] The challenges involved in achieving this improvement are significantly different compared to those in conventional photovoltaics because of the nature of the materials used. When an OPV absorbs a photon, a tightly bound exciton is formed. This exciton diffuses around the device, and if it reaches a heterojunction between electron- and hole-accepting polymers before decaying, it may dissociate to form a geminate charge pair. Typically, electron- and hole-accepting polymers are blended together to form a bulk heterojunction that facilitates efficient formation of geminate charges from excitons. Geminate charges must overcome their mutual attraction before they recombine to separate into free charges. Once separate, these free charges may still recombine bimolecularly with other free carriers *en route* to the contacts. Of these processes, it is the efficiency with which geminate pairs are separated η_{GS} that primarily limits OPV performance.[4–6] This is, in part, because poor dielectric screening $(2<\varepsilon_R<4)$ and low carrier mobilities $(10^{-3}<\mu<10^{-5}\ \mathrm{cm^2/V\,s})$ of the host polymers make carrier separation difficult. Furthermore, the bulk heterojunction morphology necessary to efficiently dissociate the excitons limits the degree of separation available to the carriers and also comprises heterojunctions that are randomly aligned to the field. Since there is the opportunity to choose polymer combinations with varying carrier mobility and morphological properties, and tune the morphology further via solvent and deposition method, it is important to characterize the effects of morphology and carrier mobility on η_{GS} and thus OPV performance.

Onsager[7] was the first to derive equations that predict the efficiency of ion dissociation including the effects of their mutual attraction and an applied electric field. Braun[8] adapted the Onsager model to include a finite recombination rate between carriers, as is found in polymer systems, by assuming the separation yield equalled the branching ratio of the Onsager separation rate and the recombination rate. This approach is not accurate since the Onsager model implicitly describes the separation rate to infinity since there is an absorbing sink at the origin. In reality, a carrier pair, which has partially separated and collapsed back to the origin, has a finite probability of separation and, hence, the Braun model underestimates the carrier separation yield. Another formulation that treats ion separation yield in systems with a finite recombination rate accurately has been reported by Sano and Tachiya.[9] However, all of the models just discussed[6–8] necessarily consider the transporting medium to be homogenous in order to make the mathematics tractable. Hence, factors which vary on the length scale of a carrier hop that influence carrier transport, such as the value of energetic disorder or morphology, cannot be treated explicitly. Monte Carlo models allow incorporation of this fine detail and have been used successfully to explain many aspects of OPV performance.[10–14]

Monte Carlo investigations of geminate pair behavior reported thus far have characterized a number of deficiencies with the Onsager–Braun approach. Barth *et al.*[14] showed that energetic disorder increases η_{GS} above that which would be expected by Onsager–Braun theory at low temperatures and

[a]Electronic mail: cg378@cam.ac.uk.

low fields simply because the geminate pair is injected with a nonequilibrium energy which assists carrier separation. Offermans *et al.*[11] later showed that polymers with differing degrees of energetic disorder also have charge separation enhanced by energy equilibration. Peumans and Forrest[13] showed that restricting electrons and holes to either side of a heterojunction can significantly affect η_{GS} when compared to an effective-medium approach, as is in Refs. 7–9.

These investigations have increased understanding of some aspects of geminate pair behavior and highlighted the inadequacies of the effective-medium approach. However, there are a number of issues suggested by experiment to be crucial in determining η_{GS} that have not been examined in the controlled environment of a Monte Carlo model. Recent experiments by McNeill *et al.*[5] showed that η_P in polyfluorene OPVs is at a maximum when the domain size is ~20 nm, which is much larger than the exciton diffusion length and so suggested that the degree of carrier separation available due to the morphology limits OPV performance. Additionally, the electron and hole mobilities of the acceptor and donor polymers are often unbalanced, which at a device level is commonly believed to produce space-charge effects[15] but has not been examined at the geminate pair level. Furthermore, little work has been reported on the dynamical behavior of the geminate pair, which is of interest since η_{GS} could be considered to be determined by the competing rates of successful separation and recombination. Nelson[16] and Offermans *et al.*[11] examined the temporal characteristics of carrier populations within OPVs but a detailed examination of the dynamics of carrier separation and recombination for individual geminate pairs is yet to be reported. In this paper we present results of detailed simulations relating domain size and heterojunction-field alignment, as well as carrier mobility, to η_{GS}. Additionally, we also examine the dynamical behavior of those carriers which successfully separate and those which recombine to give a more detailed picture of carrier transport.

SIMULATION METHODOLOGY

The Monte Carlo simulation used here is substantially similar to that reported in Ref. 12 and so will only be discussed briefly here. Polymer morphology is represented by a regular 1 nm Cartesian lattice of equal amounts electron- and hole-accepting polymer. Polymer blends with average domain sizes of $4\ \text{nm} \leqslant l \leqslant 16\ \text{nm}$ were generated by the method reported in Ref. 5. Bilayer structures of various orientations to the electric field were also examined and are referred to by the angle θ between the electric field and the normal vector of the heterojunction plane which points into the electron-accepting polymer. Individual polymer chains are not considered in the morphology, and so the hopping transport within the model represents an average behavior of intra- and inter-chain processes. In all cases the extent of the simulation volume is large compared to the thermal capture radius of the carriers, and the electric field vector is in the direction of positive z.

Each site is randomly assigned an energetic disorder picked from a Gaussian distribution of standard deviation σ prior to each trial. Thereafter a geminate pair is injected either at a random heterojunction in the case of a polymer blend or at a heterojunction at the centre of the simulation volume in the case of a bilayer. The hop rate from the current site i to an adjacent site j is calculated using a Marcus rate expression[17] in order to include polaronic effects,

$$R_{i\to j} = \upsilon_{\text{hop}} \exp\left(-\frac{(E_j - E_i + E_R)^2}{4E_R kT}\right). \tag{1}$$

Here E_i and E_j are the potential energies of the sites i and j, respectively, E_R is half the polaron relaxation energy and υ_{hop} is a prefactor that contains information about the average likelihood of tunneling between polymer chains. The site energies include electrostatic interactions between the carriers and of the external electric field ξ. Recombination between adjacent electrons and holes occurs at a constant rate R_{rec}. Hop times $\tau_{i\to j}$ are generated for the processes with rates $R_{i\to j}$ using

$$\tau_{i\to j} = -\frac{\ln(r)}{R_{i\to j}}, \tag{2}$$

where r is a random number, which is evenly distributed between 0 and 1. Of all the possible events, the one with the shortest waiting time is chosen as the behavior for that carrier. Events within the simulation are ordered using the first reaction method for computational efficiency since this technique makes little difference to carrier behavior but does give considerable savings in computational load.[12]

Successive carrier hops are performed until the geminate pair recombines or successfully separates, defined by the common assumption that the carriers are free when separated by more than the thermal capture radius,

$$r_c = \frac{q^2}{4\pi\varepsilon_0\varepsilon_R kT}, \tag{3}$$

where q is the electron charge. This simple assumption neglects the effects of entropy, which we discuss in greater detail later on in the paper. When the simulation terminates, the simulation time t is noted to build probability distribution functions (PDFs) of the time at which a successful separation event occurs $S(t)$ or the time at which a recombination event occurs $R(t)$. Simulations are repeated at least 10^4 times in order to build up reliable statistics. As well as collecting information about the eventual fate of geminate pairs, we also record information about how the separation of geminate pairs evolves prior to recombination or successful separation. At a given time during the simulation the separation of the remaining carriers d is recorded and used to build the PDF of carrier separation $X(d)$. The parameters used for the simulation are the same as those in Ref. 12, unless otherwise specified, and are repeated in Table I. While these values are not unique, they are physically reasonable and reproduce mobility with a sensible order of magnitude ($\mu \sim 2 \times 10^{-5}\ \text{cm}^2/\text{V s}$ at low fields) and blend OPV internal quantum efficiency in line with experiment.[12]

TABLE I. Parameters used in simulation (unless otherwise specified).

σ	10^{-20} J
υ_{hop}	6.76×10^{11} s^{-1}
ε_R	4
E_R	1.2×10^{-19} J
R_{rec}	5×10^{5} s^{-1}
T	298 K

DIFFERING CARRIER MOBILITIES

In an effort to isolate the effect of bulk mobility alone we choose to scale υ_{hop} in Eq. (1) by factors N_e and N_h for electrons and holes, respectively. Hereafter, we shall distinguish between devices with different mobilities via the values of N. Inevitably, this method of altering mobility does lead to some overgeneralization since carrier mobility depends on many factors unique to a material, but nonetheless it allows us to examine the effect of changing mobility on geminate pair dynamics.

Figures 1(a) and 1(b) show $S(t)$ and $R(t)$, respectively, for $\theta=0°$ bilayers comprising polymers with $N_e=N_h=1$, $N_e=N_h=10$, and $N_e=10$ and $N_h=1$ when $\xi=1.7\times10^7$ V m^{-1} (which corresponds approximately to the field in a 70 nm OPV device with 1.2 V built-in voltage at short circuit) and

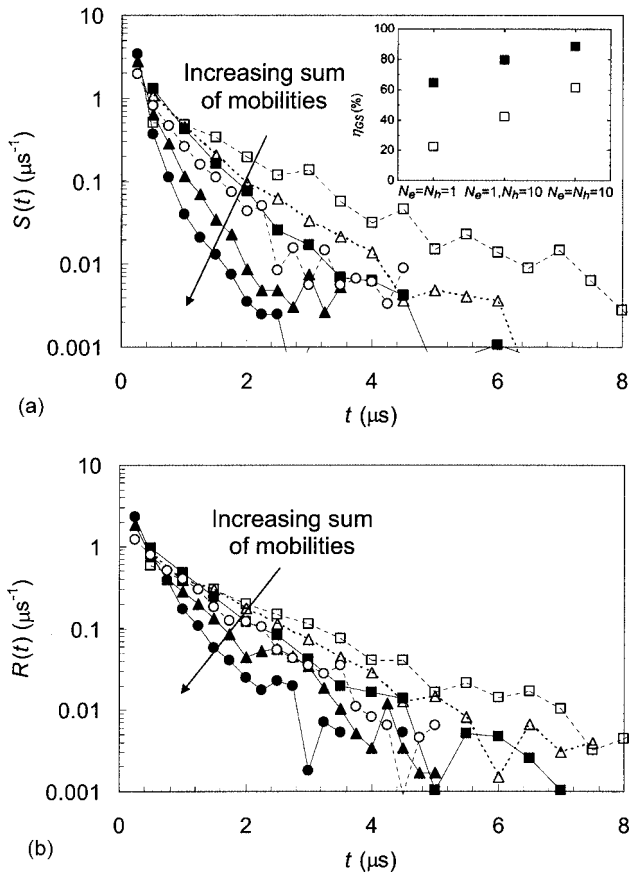

FIG. 1. The probability density function of (a) carrier separation $S(t)$ and (b) carrier recombination $R(t)$ for bilayers when $\theta=0°$ for $\xi=1.7\times10^7$ V m^{-1} (closed symbols) and $\xi=0$ V m^{-1} (open symbols), $N_e=N_h=1$ (squares), $N_e=10$ and $N_h=1$ (triangles), and $N_e=N_h=10$ (circles). Lines are a guide to the eyes. The inset in (a) shows η_{GS} for the mobility combinations when $\xi=1.7\times10^7$ V m^{-1} (closed symbols) and $\xi=0$ V m^{-1} (open symbols).

$\xi=0$ V m^{-1}. The dynamics of $S(t)$ and $R(t)$ depend on the population of geminate pairs at t and the characteristic rate at which carriers are removed by successful separation or recombination, respectively. Hence, all of the curves are peaked at short times where the population of geminate pairs is greatest, and decay away with increasing time as population reduces. The conditions for exponential decay are satisfied if the characteristic rate of loss to either mechanism is constant, which can be seen to be approximately true. Some slight variations from pure single-exponential behavior can be seen at long times when the rate of decay in $S(t)$ and $R(t)$ reduces slightly. Removing energetic disorder ($\sigma=0$) causes $S(t)$ and $R(t)$ became pure single-exponential decays. Hence, the deviation from single-exponential behavior is due to carriers equilibrating in the density of states and in doing so becoming less mobile.

Figure 1(b) shows that the average time to recombination τ_R is approximately the inverse of the recombination rate R_{rec} ($=5\times10^5$ s^{-1}) as expected but also reduces slightly with increasing sum of carrier mobilities and increasing ξ. This is because the population of carriers at a given time, which can undergo recombination, and so the number of recombination events reduces more quickly when the efficacy of the competing separation process is increased. Figure 1(a) shows that the average time to reach successful separation decreases with increasing sum of the mobilities as expected. Not resolved on the scale of Fig. 1 is the small delay of ~20 ns (~50 ns) between the origin and the peak of $S(t)$ when $\xi=1.7\times10^7$ V m^{-1} ($\xi=0$ V m^{-1}), which is indicative of the minimum time necessary for charge pair separation.

Figures 2(a) and 2(b) show the electric field dependence of η_{GS} for $\theta=0°$ bilayers when only one mobility is changed ($1\leqslant N_e\leqslant50$) with the other is kept constant ($N_h=1$), and when both mobilities are changed in unison ($1\leqslant N_e=N_h\leqslant50$). A closer inspection of Figs. 2(a) and 2(b) suggests that η_{GS} increases approximately as the average of the mobilities. This is further examined in Fig. 2(c), which shows the electric field dependence of η_{GS} when the electron mobility is increased by a factor of $1\leqslant N_e\leqslant2$, but the average mobility is kept constant, $N_h=(2-N_e)$. It can be seen that η_{GS} has a weak dependence on the larger carrier mobility when the average of the carrier mobilities is kept constant.

Importantly, Fig. 2 shows that increasing carrier mobility improves η_{GS} most markedly at lower fields, suggesting that OPV maximum power output may also increase. However, increasing only one mobility may lead to space-charge limited photocurrent in a device context.[15] To test whether increased η_{GS} translates to higher OPV performance, current-voltage curves for a 70 nm OPV blend device with an average feature size of 4 nm, with unequal ($N_e=10$ and $N_h=1$) and equal ($N_e=N_h=1$ and $N_e=N_h=10$) mobilities, were simulated at an injection rate of geminate pairs of 8×10^{14} s^{-1} mm^{-2} (which corresponds approximately to 1 sun irradiance assuming that the photon to geminate pair conversion ratio is 25%). The injection barriers were assumed to be 0.4 eV for both electrons and holes, and the built-in voltage is 1.2 V. Increasing one ($N_e=10$ and $N_h=1$) or both ($N_e=N_h=10$) mobilities led to corresponding increases in the maximum power output by 75% and 110%,

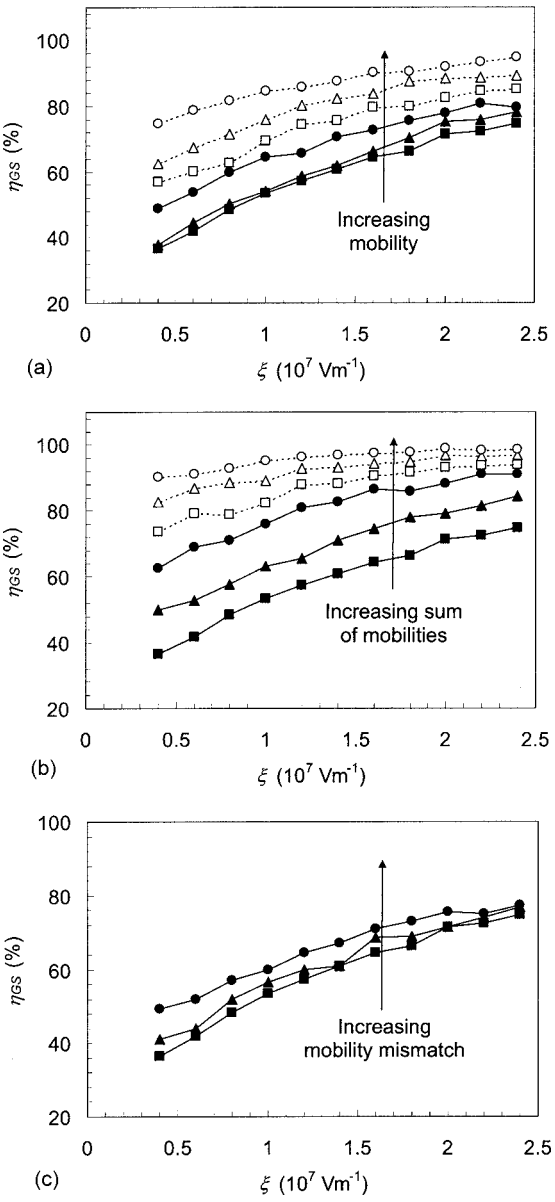

FIG. 2. Predicted η_{GS} for $\theta=0°$ bilayers as a function of applied field ξ when (a) $N_e=1$ (closed squares), 2 (closed triangles), 5 (closed circles), 10 (open squares), 20 (open triangles), and 50 (open circles) while $N_h=1$, (b) $N_e=N_h=1$ (closed squares), 2 (closed triangles), 5 (closed circles), 10 (open squares), 20 (open triangles), and 50 (open circles), and (c) $N_e=N_h=1$ (squares), $N_e=1.1$ and $N_h=0.9$ (triangles), and $N_e=2$ and $N_h=0$ (circles).

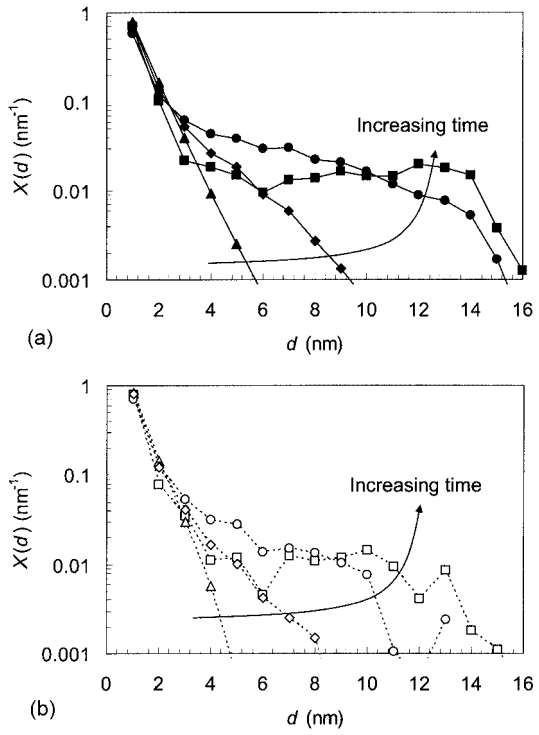

FIG. 3. The probability density function of carrier separation for carriers yet to recombine or separate, $X(d)$ for $t=5$ ns (triangles), 25 ns (diamonds), 50 ns (circles), and 500 ns (squares) when (a) $\xi=1.7\times10^7$ V m^{-1} and (b) $\xi=0$ V m^{-1}. Lines are a guide to the eyes. In this simulation the structure considered is a $\theta=0°$ bilayer.

respectively, compared to that for a similar device with $N_e=N_h=1$. It should be noted that this is not a strenuous test of space-charge effects; however, it shows that OPV performance can increase with carrier mobility even if the resultant mobilities are unbalanced.

GEMINATE PAIR SEPARATION DYNAMICS

Figure 1(a) shows that η_{GS} does not equal the branching ratio of the separation rate to recombination rate, $\tau_R/(\tau_S+\tau_R)$ and, hence, that the populations of carriers which eventually recombine or separate are statistically independent. Intuitively, we can ascribe this behavior to carriers in the process of separating experiencing a smaller Coulombic interaction than that of tightly bound carriers, which eventually recombine. Examining the behavior of recombining carriers more closely, we can deduce that the number of carriers available for recombination is continually being reduced by separation since τ_R decreases with increasing mobility or increasing field. It is interesting to ask if the energetic disorder of the dissociation site is primarily responsible for whether a geminate pair dissociates or not since one could imagine that energetic disorder may lead to trapping of the pair close to the interface. To investigate this further, we measured the distance traveled by the "center of mass" of a geminate pair in the plane of the heterojunction for geminate pairs that recombine. It was found that the rms displacement of a recombining geminate pair in the plane of the heterojunction was 26 nm when $\xi=1.7\times10^7$ V m^{-1} and $N_e=N_h=1$ for a $\theta=0°$ bilayer; hence, the dissociation site appears to play little role in the eventual fate of a geminate pair for this model system.

The dynamical behavior of separating carriers is shown in Figs. 3(a) and 3(b), which show the PDFs $X(d)$ for $\theta=0°$ bilayers when 5 ns$\leqslant t\leqslant$500 ns at fields of $\xi=1.7\times10^7$ V m^{-1} and $\xi=0$ V m^{-1}, respectively. It can be seen for both values of ξ and for all t that carriers are strongly localized due to the Coulombic attraction between carriers. Figure 4 shows η_{GS} for those carriers that remain in the simulation at 100 ns (i.e., after $X(d)$ has reached the steady state) as a function of d for a range of ξ. Generally, it can be seen that η_{GS} increases with d, as one might expect. However, when a separating field is applied, η_{GS} increases sharply when $d\sim3$ nm. This shows that geminate pairs can effectively avoid

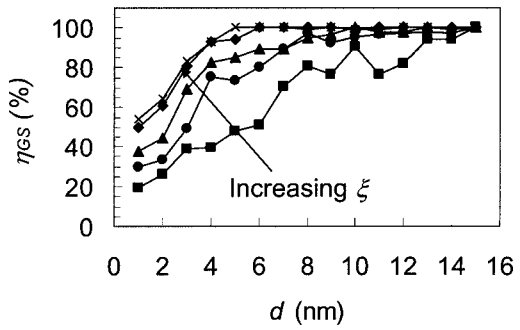

FIG. 4. η_{GS} as a function of separation d for geminate pairs present in the simulation after 100 ns when $\xi=0$ V m^{-1} (squares), 5×10^6 V m^{-1} (circles), 10^7 V m^{-1} (triangles), 2×10^7 V m^{-1} (diamonds), and 2.4×10^7 V m^{-1} (crosses). In this simulation the structure considered is a $\theta=0°$ bilayer.

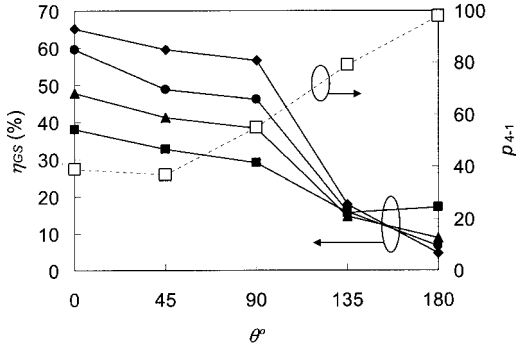

FIG. 5. Solid symbols show the predicted η_{GS} at an electric field of $\xi=1.7\times10^7$ V m^{-1} (diamonds), 1.3×10^7 V m^{-1} (circles), 9×10^6 V m^{-1} (triangles), and 5×10^6 V m^{-1} (squares) when $N_e=1$ and $N_h=1$ for bilayers as a function of heterojunction angle θ. Open symbols show the probability of a geminate pair with separation of 4 nm or greater collapsing back to a separation of 1 nm, $p_{4\to1}$ when $\xi=1.7\times10^7$ V m^{-1}, and $N_e=1$ and $N_h=1$, as a function of heterojunction angle θ. Lines are a guide to the eyes.

recombination even when they have achieved separations smaller than r_c (=16 nm here), and that the tail in $X(d)$ comprises mostly carriers which are *en route* to separation. A geminate charge pair can become effectively free at separations smaller than r_c as charge dissociation is accompanied with a significant increase in entropy of similar energetic value to the Coulombic attraction.[18] Consequently, one may expect that η_{GS} in a blend would only be affected by the degree of separation available within the morphology when the domain size is less than ~4 nm. Hence it is necessary to look more closely at the mechanism given in Ref. 5 explaining why blend OPVs have maximum η_P when the domain size is ~20 nm. We discuss this in more detail in the next section.

The peak in $X(d)$ at low d observed over the field range considered in Fig. 3 may seem at odds with the results of Offermans *et al.*,[11] who showed in a $\theta=90°$ bilayer that the mean distance of carriers away from the heterojunction increased as the field decreased. However, Offermans *et al.*[11] measured the mean distance of all carriers in the device to the heterojunction, and so the population measured contained carriers that are yet to separate, considered here, and carriers that have already successfully separated. The population of separated carriers will move more diffusively as the field reduces and may account for the difference in results.

POLYMER MORPHOLOGY

We first examine the effect of heterojunction alignment to an applied field upon geminate pair behavior. Figure 5 shows η_{GS} for a bilayer comprising materials with equal mobilities ($N_e=N_h=1$) as a function of θ when 5×10^6 V m^{-1} $\leqslant\xi\leqslant1.7\times10^7$ V m^{-1}. For a given value of electric field, η_{GS} decreases as θ increases since the space in which the carriers can execute their random walk, which is biased in the direction of the field becomes more constrained. It can be seen that η_{GS} increases with increasing field when $\theta<135°$ and reduces with increasing field when $\theta>135°$. Quantitatively, it can be seen that η_{GS} is little affected by an increase in θ from 0° to 90° and drops significantly at higher angles. This shows that OPVs with fine phase separation, which contain a mixture of heterojunction orientations, suffer significant reductions in η_{GS} compared to a bilayer comprising the same materials in agreement with Ref. 11. However, OPVs with interdigitated phases, such as in Ref. 19, would by contrast have geminate pair separation performance very similar to that of a bilayer using the same materials, while having much greater interfacial area to assist exciton dissociation. Figure 6 shows $S(t)$ for a bilayer with equal mobilities ($N_e=N_h=1$) when $0°\leqslant\theta\leqslant180°$ and $\xi=1.7\times10^7$ V m^{-1}. It can be seen that, as with η_{GS}, the dynamical behavior of the geminate pair is not much altered by increasing θ from 0° to 90° and thereafter the dynamics of escape become slower. The increase in average time to successful separation for $\theta>90°$ is due to a component of the field pushing the carriers toward the interface, making separation a more arduous and slower process. The pdf $R(t)$ shows similarly slower dynamical behavior as θ increases. The PDFs $X(t)$ when 500 ns $\leqslant t\leqslant10$ μs and $0°\leqslant\theta\leqslant180°$ show that θ does not affect the general shape of the PDF (as in Fig. 2) but does suppress the tail of the distribution by up to an order of magnitude as θ increases to 180°.

In Fig. 7 we show η_{GS} for blend morphologies with 4 nm$\leqslant l\leqslant$16 nm over a wide range of electric fields 0 V m$^{-1}\leqslant\xi\leqslant9.5\times10^7$ V m^{-1}. As expected, η_{GS} increases with ξ, eventually saturating when $\xi\sim9\times10^7$ V m^{-1}. It is interesting to note that the blend morphology promotes competition between separation and recombination over a much wider field range when compared to a bilayer, for which η_{GS}

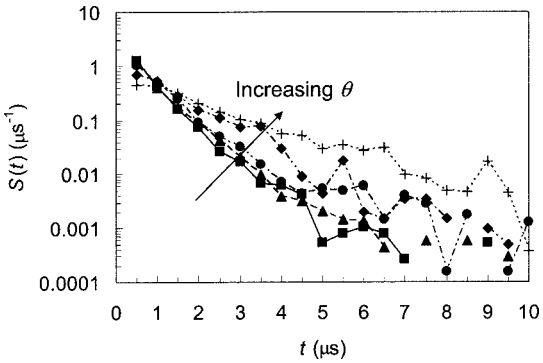

FIG. 6. $S(t)$ when $N_e=1$ and $N_h=1$ and $\xi=1.7\times10^7$ V m^{-1} for bilayers with $\theta=0°$ (squares), 45° (triangles), 90° (circles), 135° (diamonds), and 180° (crosses).

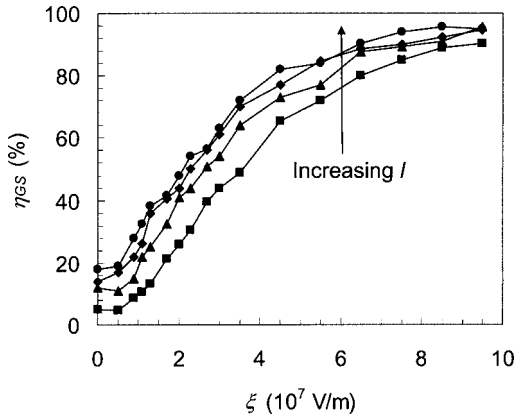

FIG. 7. Average η_{GS} as a function of ξ for a polymer blend with domain sizes, l=4 nm (squares), 8 nm (triangles), 12 nm (diamonds), and 16 nm (circles).

saturates at $\xi \sim 2.5 \times 10^7$ V m^{-1} (Fig. 2). Further, η_{GS} is shown to approach 100% even though the blend morphologies contain heterojunctions which are incorrectly aligned to the field. Reducing the temperature led to a significant reduction in the value at which η_{GS} saturates with increasing field. This shows that dissociation efficiency at 298 K can approach 100% since the geminate charges have sufficient thermal energy to diffuse to a more favorably aligned heterojunction over which field-assisted dissociation is possible.

Generally, blend morphologies at a given ξ have lower η_{GS} than the solid angle average of the corresponding η_{GS} curve in Fig. 5, showing that the limited space to separate imposed by the morphology limits η_{GS} beyond that expected from the random orientation of heterojunctions. Figure 7 also shows that η_{GS} increases with domain size l and begins to saturate when the domain size increases to $\sim$16 nm, in agreement with Ref. 5. In the previous section, we showed that successful charge separation can occur in a bilayer over distances smaller than r_c, and this is because charge separation is associated with an increase in entropy comparable to the Coulombic binding energy.[18] We may therefore expect that η_{GS} would increase with domain size and begin to saturate before the domain size reaches r_c but this is not seen here. We explain this result as follows. In a bilayer, a carrier can become effectively free over short distances since carriers have an infinite hemispherical volume into which it can drift and diffuse. In a blend the domains impede percolation of carriers away from one another, making it more likely that geminate charges will come again into close proximity. As the domain size increases, the geminate charges can percolate away from one another more easily and so η_{GS} increases.

We examine how domain size affects the recombination probabilities of carriers that have partially separated by defining, $p_{4\to1}$, which is the probability of a geminate pair having achieved a separation of 4 nm or more collapsing back to a separation of 1 nm. Hence, the quantity $p_{4\to1}$ is indicative of the recombination probability of geminate charges that are partially separated. Figure 5 shows $p_{4\to1}$ for a bilayer when $\xi = 1.7 \times 10^7$ V m^{-1} and $N_e = N_h = 1$, as function of θ. As might be expected, $p_{4\to1}$ increases with θ since carrier separation becomes more difficult. The solid angle average of this curve is 58%, which compares to $p_{4\to1}$ in a blend with l=4 nm, for the same field and mobilities, of 74%. This shows that limiting the routes to separation in a blend when compared to a bilayer concomitantly increases the recombination probability, even for carriers that have partially separated. Figure 7 shows that η_{GS} increases with domain size until it begins to saturate at $l \sim 16$ nm, suggesting that the domains in this blend are sufficiently large as to not significantly limit the possible routes to successful geminate charge separation. Indeed, we find this to be the case as $p_{4\to1}$ =60% for the l=16 nm blend, which corresponds closely to the solid angle average of $p_{4\to1}$ for bilayer structures of 58%.

CONCLUSIONS

Monte Carlo simulations have shown that geminate charge pairs in polymer-polymer photovoltaics can effectively avoid recombination by achieving separations which are smaller than the thermal capture radius. Improvement in carrier mobilities was shown to increase η_{GS} more at low fields, which in turn translates to substantial increases in maximum power output of 75% and 110% when either one or both carrier mobilities, respectively, are increased by a factor of 10. The effect of changing heterojunction-field alignment and polymer domain size on η_{GS} was also examined. Examining the charge dissociation behavior in bilayers, however, showed that geminate charges can effectively avoid recombination by achieving separations of approximately 4 nm. However, it was shown that domain sizes below $\sim$16 nm reduced η_{GS} below that which would be expected by simply averaging η_{GS} for a series of bilayers having different heterojunction-field alignments, in agreement with experimental investigations.[5] It is shown that blend morphology limits the possible routes to charge separation, explaining why there is a difference in the separation behavior between blends and bilayers.

ACKNOWLEDGMENTS

This project was supported by EU integrated project NAIMO (No. NMP04-CT-2004-500355). The authors would also like to acknowledge Dr. L. J. A. Koster and Dr. C. R. McNeill of the Cavendish Laboratory, Cambridge, UK, for helpful discussions.

[1] C. R. McNeill, A. Abrusci, J. Zaumseil, R. Wilson, M. J. McKiernan, J. H. Burroughes, J. J. M. Halls, N. C. Greenham, and R. H. Friend, Appl. Phys. Lett. **90**, 193506 (2007).
[2] S. C. Veenestra, J. Loos, and J. M. Kroon, Prog. Photovoltaics **15**, 727 (2007).
[3] M. Ganstrom, K. Petritsch, A. C. Arias, A. Lux, M. R. Andresson, and R. H. Friend, Nature (London) **395**, 257 (1998).
[4] C. Yin, T. Kietzke, D. Neher, and H.-H. Hörhold, Appl. Phys. Lett. **90**, 092117 (2007).
[5] C. R. McNeill, S. Westenhoff, C. Groves, R. H. Friend, and N. C. Greenham, J. Phys. Chem. C **111**, 19153 (2007).
[6] R. A. Marsh, C. R. McNeill, A. Arbrusci, A. R. Campbell, and R. H. Friend, Nano Lett. **8**, 1393 (2008).
[7] L. Onsager, Phys. Rev. **54**, 554 (1938).
[8] C. L. Braun, J. Chem. Phys. **80**, 4157 (1984).
[9] H. Sano and M. Tachiya, J. Chem. Phys. **71**, 1276 (1979).
[10] P. K. Watkins, A. B. Walker, and G. L. B. Verschoor, Nano Lett. **5**, 1814 (2005).

[11] T. Offermans, S. C. J. Meskers, and R. A. J. Janssen, Chem. Phys. **308**, 125 (2005).
[12] R. A. Marsh, C. Groves, and N. C. Greenham, J. Appl. Phys. **101**, 083509 (2007).
[13] P. Peumans and S. R. Forrest, Chem. Phys. Lett. **398**, 27 (2004).
[14] S. Barth, D. Hertel, Y.-H. Tak, H. Bässler, and H. H. Hörhold, Chem. Phys. Lett. **274**, 165 (1997).
[15] V. D. Mihailetchi, J. Wildeman, and P. W. M. Blom, Phys. Rev. Lett. **94**, 126602 (2005).
[16] J. Nelson, Phys. Rev. B **67**, 155209 (2003).
[17] R. A. Marcus, Rev. Mod. Phys. **65**, 599 (1993).
[18] H. Okhita, S. Cook, Y. Astuti *et al.*, J. Am. Chem. Soc. **130**, 3030 (2008).
[19] A. B. F. Martinson, A. M. Massari, S. J. Lee, R. W. Gurney, K. E. Splan, J. T. Hopp, and S. T. Nguyen, J. Electrochem. Soc. **153**, A527 (2006).